Int. J. Nanosci. Nanotechnol., Vol. 9, No. 2, June 2013, pp. 71-76

Sintering Behavior of Porous Nanostructured Sr-Doped Lanthanum Manganite as SOFC Cathode Material

H. Tamaddon*, A. Maghsoudipour

Ceramics Department, Materials and Energy Research Center, Tehran, I. R Iran

(*) Corresponding author: tmdn.imn.86@gmail.com
(Received:19 Feb. 2013 and Accepted: 15 June 2013)

Abstract:
The fuel cells are distinguished as generating of green allocable energy and are electrochemical devices of low environmental impact. Porous nanocrystalline strontium-doped lanthanum manganite $La_{0.8}Sr_{0.2}MnO_3$ (LSM) cathode materials were prepared by mechanochemical route in various grinding times. Carbon black was employed to produce pores. The formation of LSM single phase was studied by X-ray diffraction patterns. Porosity and density amounts were measured by means of Archimedes method, furthermore, contraction of sintered samples was comparably evaluated. Scanning electron microscopy (SEM) images were used for morphological study. It is shown that the open and total porosity generally decrease with sintering temperature, however the milling time increase these factors. Relying on open porosity amount and distribution, relative density and microstructural scrutiny the proper sintering temperature was determined. The microstructural investigation indicates that the grains grow as the sintering temperature increases which leads to decrease the number of the open pores.
Keywords: *SOFC, LSM, Mechanochemical Synthesis, Cathode, Sintering Trend.*

1. INTRODUCTION

The fuel cells are distinguished as generators of distributed energy and are electrochemical devices of low environmental impact. As one of the key materials of solid oxide fuel cells (SOFCs) the cathode materials are extensively studied [1]. Among the cathode materials, $(La,Sr)MnO_3$ based perovskites due to their good chemical and thermal stability, high electrocatalytic activity for oxygen reduction at high temperatures, thermal expansion coefficient similar to the electrolyte (yttria stabilized zirconia) and high electrical conductivity are the most widely investigated materials for solid oxide fuel cells [2].
Different synthesis methods have been developed for production of LSM powders, such as solid-state reaction, sol–gel technique, hydrothermal synthesis, co-precipitation, citrate (pechini process) and combustion [3]. The solid-state reaction is an uncomplicated and single-step method of ceramic processing, which usually involves high temperatures and leads to nano-sized particles as well as rather high chemical homogeneity [4]. The optimum sintering temperature of LSM cathode is impressively depended on the synthesis procedure. In a general aspect the firing temperature of chemically prepared products [3,5-7] is lower than those of mechanochemical routes [8,9]. This paper shows that the sintering manner of the LSM cathode material must also be considered and its relevant criteria needs to be still researched.

2. EXPERIMENTAL

MnO_2, La_2O_3, and SrO (Merck, with purity > 99.9%) were used as starting reagents. MnO_2 was heated at 600 oC for 12 hours in order to convert it into Mn_2O_3. The formation of single-phase Mn_2O_3 was confirmed by X-ray powder diffraction before its use. After that the proper weight ratio of dried reactants: La_2O_3, Mn_2O_3, MnO_2, and SrO were completely mixed in aceton liquid media with an appropriate stoichiometric ratio as per reaction 1 [8].

$$0.4(La_2O_3+Mn_2O_3)+0.2(SrO+MnO_2) = La_{0.8}Sr_{0.2}MnO_3 \quad (1)$$

The principle stage of fabrication method was carried out by means of a planetary ball mill (PMV2, Tajhizceram co.). The batch of 50 gr of the aforementioned mixture was taken into the zirconia bowl. Later, 15-mm diameter zirconia balls were added into it as ball/powder ratio was 15. The rotational speed of the planetary mill was 300 rpm (revolution per minute). Finally, after sampling in different grinding times (0,3,12,24,36 and 48 hours) the ground samples were calcinated at 600°C for 2 hours in air for completing the phase formation process as well as remove the possibly absorbed moisture and impurities.

The LSM phase formation was determined by XRD diffractometry test (Philips. Pw 3710 mpd control). Then the pellet samples were obtained in the form of circular discs of 13 and 1.4-mm in diameter and thickness, respectively, by pressing the well-ground powder uniaxially at 300 MPa using hydraulic press. Carbon black in 12% wt was applied as pore former agent.

Subsequently, these green compressed speci-mens were sintered at various temperatures (1050, 1100, 1150, 1200 and 1300) with constant heating rate of 10°C/min for 4 hours. After the firing procedure the porosity and density amount of porous pellets measured with Archimedes method [10]. Finally the morphology and microstructure of sintered pellets at three various temperatures was investigated by SEM (S360 Cambridge, 1990) image analysis.

3. RESULTS AND DISCUSSION

3.1. X-ray powder diffraction

The diffraction patterns of not-milled and milled powder samples which calcinated at 600°C are illustrated in Figure 1. As can be seen diffracted

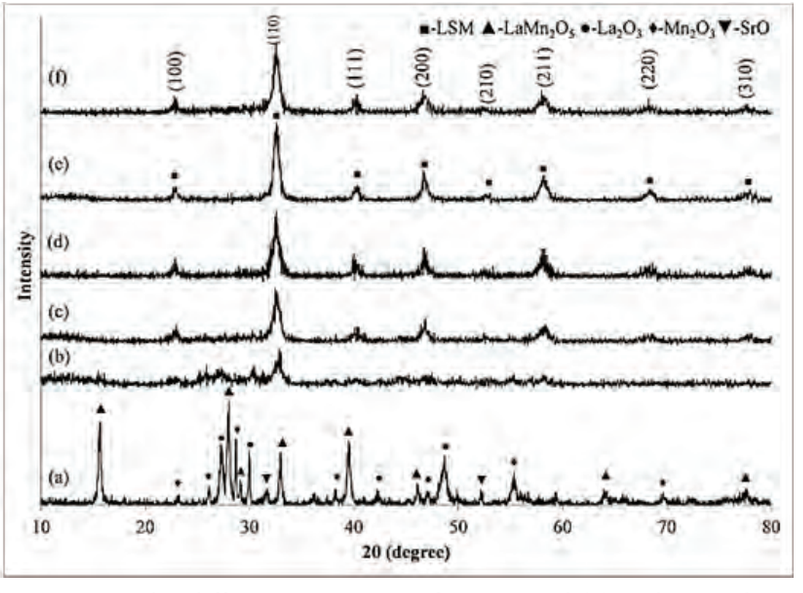

Figure 1: *X-ray powder diffraction patterns of not ground (a) and ground samples in 3 h (b), 12 h (c), 24 h (d), 36 h (e) and 48 h (e)*

lines of not ground powder sample just according with primary oxide ingredients. For the samples which milled for 12 hours and more, compared with ideal perovskite $LaMnO_3$ pattern (JCPDS: 75-440) the diffraction peaks indexed well to single phase LSM with perovskite structure and cubic symmetry. This phase formation process was completed along with grinding time increase which suggested that Sr^{2+} is successfully incorporated into the A-site (La situations) of the LSM lattice.

The milling operation causes the decrease in the mean crystallite size, also the d values vary with grinding time which is possibly ascribed to the introduction of substitution-induced non-stoichiometric defects into the perovskite lattice. Furthermore the strontium as a relatively large dopant is expected to expand the lattice parameter. As a result the d value increase.

The peak broadening in XRD patterns confirm the grain size reduction down to 10.4 nm which reported in Table 1.

Table 1: *The positions and d values corresponding to the strongest peaks and the mean crystallite sizes of milled LSM powder samples*

milling time (hour)	2θ (degree)	d (A^o)	grain size (nm)
12	32.6058	2.74406	13.5
24	32.5444	2.74909	13.1
36	32.5844	2.74581	12.4
48	32.5676	2.74719	10.4

3.2. Sintering trend

The dependency of open and total porosity of the sintered samples on the sintering temperature is clearly shown in Figure 2, 3 respectively. It can be obviously found that this factor reciprocally vary with sintering temperature, however the grinding time of mechanochemically synthesized samples has a direct influence on porosity level.

As the firing temperature increases the open porosity of porous pellets generally varies with an downward trend, especially in the range of 1100-1300°C. This trend can be confirmed by comparing with the relative density curves which illustrated in Figure 4.

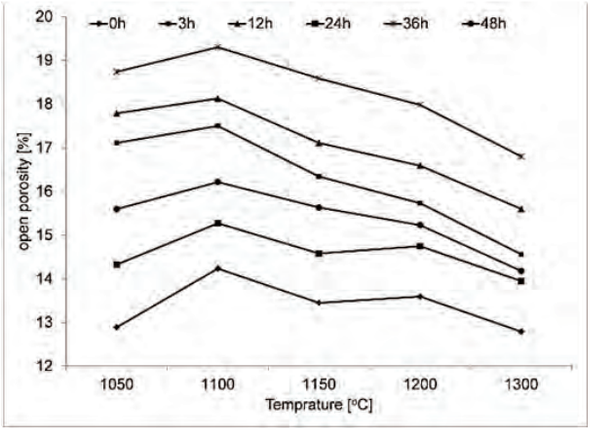

Figure 2: *Variation of open porosity as a function of sintering temperature and grinding time*

The most important point in this Figure is the reduction of density with milling time increase. The 36 h ground sample which sintered in 1300°C has the greatest open porosity and lowest relative density amount. This case can be selected as optimum sample due to the necessity of open porosity presence in cathode materials in order to O_2 reduction and fuel transportation.

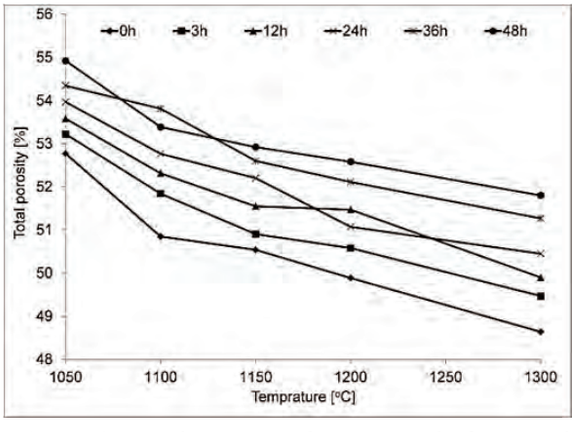

Figure 3: *Total porosity change trend of sintered pellets by various temperatures*

Base on the comparison between size contraction percent amounts which are shown in Figure 5, it reveals that the milling process enormously affect

on the trend as well as quantity of this factor. As can be seen along with the grinding time increase the contraction percent has been grown, also the temperature dependency of this property is ascending which may be interpreted by particle size decrease and suitable distribution due to the milling procedure.

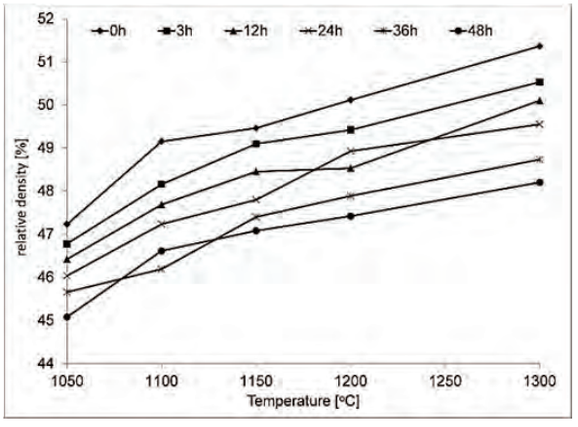

Figure 4: *Temperature dependence of relative density for the LSM ground samples in different milling times*

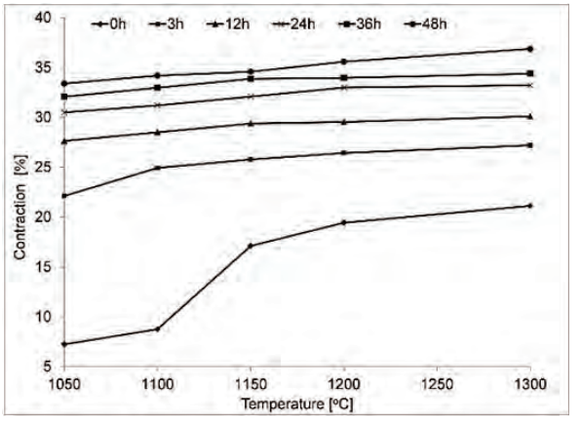

Figure 5: *Contraction rate of sintered samples as a function of sintering temperature*

3.3. Morphology

In comparison with anode electrode, the study of the microstructure of cathode electrode surface is somewhat more difficult due to its materials composition, much finer microstructure and presence of open as well as closed porosities [11]. Figure 6 gives the SEM images of the surface of the 36 h ground samples sintered at different temperatures.

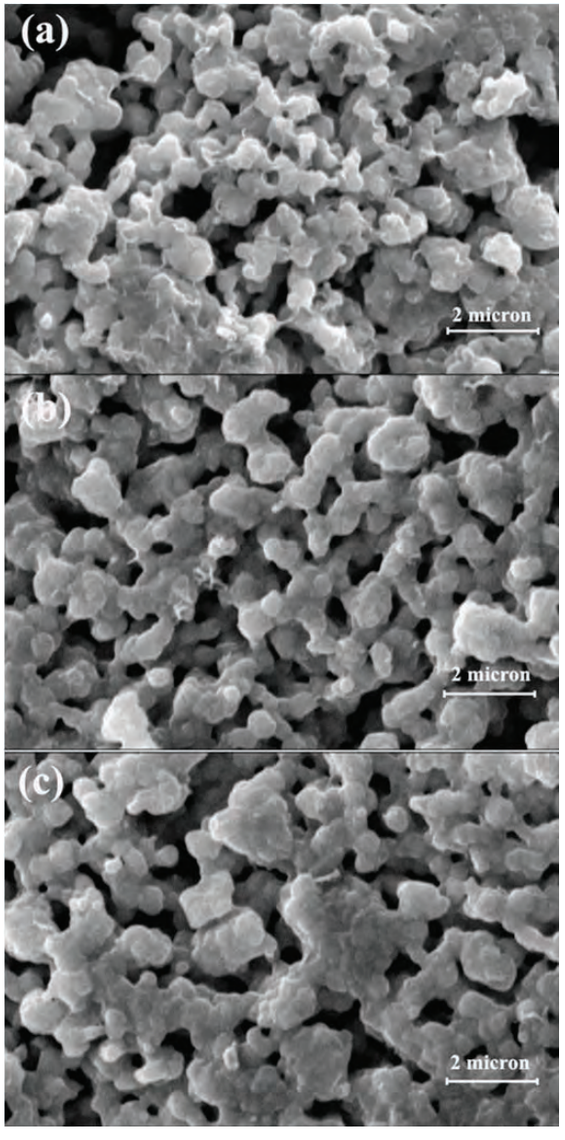

Figure 6: *Comparison of scanning electron microphotographs of sintered porous pellets at 1100 (a), 1200 (b) and 1300°C (c)*

Evidently, with increasing the sintering temperature, the grains growth occur and the number of the open pores reduces, however the volume and size of these pores increase. On the other hand the open pores are located at multi-grain boundaries. At sintering temperature of 1100°C the open porosities are well distributed but the sintering process has not been completed as the observed necking phenomenon between grains certify it. The higher

temperature is, the larger the volume of the open pores is, specifically the sample sintered at 1300°C. At this firing temperature there is an adherent microcrostructure with an optimum pore size and amount.

4. CONCLUSION

Considering the comprehensive properties, it is suggested that the proper sintering temperature is 1300°C, however the optimum milling time in order to reach the maximum amount of open porosity is 36 h. The effect of milling process in sintering behavior improvement is to produce the nano-sized LSM cathode samples with more open porosity along with well distribution.

ACKNOWLEDGMENT

This technical effort was performed in support of Materials and Energy Research Center (MERC)

REFERENCES

1. G. J. Li, Z.R. Sun, H. Zhao, C.H. Chen, R.M. Ren: Ceram. Int., Vol. 33, (2007), pp. 1503-7.
2. S. P. Jiang: J. Power Sources, Vol. 124, (2003), pp. 390-402.
3. L.D. Conceicao, C.R.B. Silva: Mater. Charact., Vol. 60, (2009), pp. 1417-23.
4. Bolarin AM, Sanchez F, Ponce A, Martinez EE. Mechanosynthesis of lanthanum manganite. Mater. Sci. Eng., A, Vol. 454-455, (2007), pp. 69–74.
5. A. Kumar, P.S. Devi, H.S. Maiti: J. Power Sources, Vol. 161, (2006), pp. 79–86.
6. F. Zheng, L.R. Pederson: J. Electrochem. Soc., Vol. 146, No. 8, (1999), pp. 2810-16.
7. R. Chiba, F. Yoshimura, Y. Sakurai, Y. Tabata, M. Arakawa: Solid State Ionics, Vol. 175, (2004), pp. 23-27.
8. K.R. Nagde, S.S. Bhoga: Ionics, Vol. 16, (2010), pp. 361-70.
9. N. Hobara, K. Takizawa, A. Hagiwara, K. Sato, H. Abe, M. Naito: Adv. Powder Technol., Vol. 22, (2011), pp. 102-7.
10. B.H. Drive, W. Conshohocken: ASTM Standards Handbook, C373 standard number, United states (1999), pp. 118-119.
11. A. Lanzini, P. Leone, P. Asinari: J. Power Sources, Vol. 194, (2009), pp. 408-22.